Pharmaceutical Research, Vol. 25, No. 9, September 2008 (© 2008)
DOI: 10.1007/s11095-008-9591-6

Research Paper

Characterization of Polyion Complex Micelles Designed to Address the Challenges of Oligonucleotide Delivery

Marie-Hélène Dufresne,[1] Mahmoud Elsabahy,[1] and Jean-Christophe Leroux[1,2]

Received February 15, 2008; accepted April 3, 2008; published online May 2, 2008

Purpose. To optimize oligonucleotide (ODN)-based polyion complex micelles (PICMs) by studying the effects of polymer composition and length on their properties.
Methods. Atom transfer radical polymerization was used to synthesize copolymers with increasing hydrophilic nonionic and cationic block lengths. PICMs were prepared by mixing the copolymers and ODN at various nitrogen-to-phosphate (N/P) ratios and characterized by gel electrophoresis and dynamic light scattering. The stability of the complexes towards dissociation was tested using a competitive assay with heparin. Finally, protection of the incorporated ODN against DNAse I degradation was evaluated.
Results. A library of copolymers composed of poly(ethylene glycol) (PEG) and poly(aminoethyl methacrylate) (PAEMA) and/or poly((dimethylamino)ethylmethacrylate) (PDMAEMA) was synthesized. All polymers efficiently interacted with the ODN at N/P ratios approaching 1.5. Narrowly distributed but easily dissociable PICMs were obtained using PEG 5000 and short DMAEMA chains. Shortening the PEG block to 2000, increasing the number of cationic units and using AEMA produced more stable complexes but at the cost of colloidal properties. All polymers were able to protect the ODN from nuclease degradation.
Conclusions. PEG 3000-based PICMs possess good colloidal properties, intermediate stability towards dissociation and adjustable buffering capacity, making them potentially useful for the delivery of nucleic acid drugs.

KEY WORDS: atom transfer radical polymerization; (dimethylamino)ethyl methacrylate; oligonucleotide; polymeric micelles; polymer composition.

INTRODUCTION

The use of nucleic acids such as plasmid DNA, antisense oligonucleotides (ODNs) or small interfering RNAs (siRNAs) is an elegant approach to treat numerous diseases spanning from infections (1) to cancer (2) to genetic anomalies (3,4). Its success, however, is greatly limited by the inherent physicochemical properties of the genetic material to be delivered. It is now broadly recognized that the rapid degradation of these molecules by nucleases (5,6), their short blood half-life (7) and inadequate entry into cells (8) call for the chemical modification of the nucleic acids (9) and/or the utilization of specialized delivery systems (10–13).

Polyion complex micelles (PICMs) decorated with a targeting ligand are conceptually one of the best vehicles available thus far for the delivery of nucleic acid drugs. PICMs result from cooperative electrostatic interactions between the genetic material and a cationic copolymer presenting a water-soluble nonionic segment. Upon complexation, the charge-compensated nucleic acid/cationic chains self-assemble into a micellar core while the hydrophilic segments form a protecting corona (14,15). The corona not only confers solubility and colloidal stability to the system but also shields any cationic charges. Complexes with surface cationic charges are known to unspecifically interact with blood components and non-target cells, leading to short blood half-life and toxicity when *in vivo* applications are sought (16,17).

If a lot of insight on the physicochemical properties of complexes and transfection efficiency has been gained by studying the interaction of plasmid DNA with cationic polymers, it appears that the extrapolation of this knowledge to the various genetic materials (such as siRNAs, ODNs, *etc.*) does not always hold. For instance, the effects of poly(ethylene glycol) (PEG) chain length and density on the physicochemical properties and transfection efficiency of complexes based on branched poly(ethyleneimine) (PEI)-*graft*-PEG were shown to vary whether the genetic material used was plasmid DNA (18), phosphodiester ODN (19) or siRNA (20). Likewise, the *in vitro* performance of a branched PEI of particular molecular weight (MW) was affected

[1] Faculty of Pharmacy, University of Montreal, P.O. Box 6128, Downtown Station, Montreal, Quebec H3C 3J7, Canada.
[2] To whom correspondence should be addressed. (e-mail: Jean-Christophe.Leroux@umontreal.ca)

ABBREVIATIONS: AEMA, 2-aminoethyl methacrylate; AEMABoc, 2-(*N*-(*tert*-butoxycarbonyl)amino)ethyl methacrylate; ATRP, atom transfer radical polymerization; *β*, buffering capacity; DLS, dynamic light scattering; DMAEMA, 2-(*N*,*N*-dimethylamino) ethyl methacrylate; EDTA, ethylenediaminetetraacetic acid; EO, ethylene oxide; EtBr, ethidium bromide; GPC, gel permeation chromatography; ^{1}H NMR, proton nuclear magnetic resonance; M_n, number-average molecular weight; M_w, weight-average molecular weight; MW, molecular weight; N/P, nitrogen-to-phosphate; ODN, oligodeoxyribonucleotide; PEG, poly(ethylene glycol); PEI, poly (ethyleneimine); PI, polydispersity index; PICMs, polyion complex micelles; siRNA, small interfering RNA; SD, standard deviation; THF, tetrahydrofuran.

by the chemistry of the ODN used (phosphodiester *vs.* phosphorothioate) (21). Differences in the interactions between ODNs of various structures (linear or hairpin structured ODNs) and a polymer have also been reported (22).

In the same way, all polymers cannot be expected to interact similarly with the genetic material. For instance, it has been shown that a single atom modification could greatly influence the strength of the interactions between a polymer and DNA, thereby affecting the properties of the complexes and transfection efficiency (23,24). Variations in the strength of the interaction between polymer and DNA also arise depending on the substitution on the amino group (*i.e.* primary *vs.* tertiary *vs.* quaternary) (25,26). Furthermore, the balance between the nonionic hydrophilic and the cationic chain lengths greatly contributes to the properties of the complexes and to their transfection efficiency. In a systematic study, Lam *et al.* have observed higher condensation of plasmid DNA and improved transfection efficiency for polymers with increasing cationic segments (27). However, this was at the cost of colloidal properties. Clearly, the intrinsic physicochemical properties (MW, hydrophilic nonionic/cationic balance, aqueous conformation, density of charges, *etc.*) of both the nucleic acid and polymer will promote different interactions and affect the performance of the complexes. This strongly evidences the need to optimize a gene delivery system for a specific genetic material/polymer pair.

In line with the above statement, the aim of this work was to optimize *phosphorothioate* ODN-based complexes by studying the effects of polymer composition and length on their properties. We selected an ODN with the *phosphorothioate* chemistry as it remains one of the most widely employed and successful chemical modification of ODNs, conferring high stability to the ODN without compromising its mechanism of action (9). Derivatives of 2-aminoethyl methacrylate (AEMA) were in turn chosen to make up the cationic segment because of their facile controlled polymerization (28–30) and commercial availability as different order amines. These two aspects are exploited herein to prepare a 33-member block copolymer library in which the chain length and buffering capacity of the polymers are methodically varied. To the best of our knowledge, there is only one other study dealing with the optimization of PICMs of a *phosphorothioate* ODN and an AEMA derivative (31). Specifically, Desphande *et al.* looked at the effects of the architecture (linear, brush or comb) of copolymers of PEG and 2-(*N*,*N*-dimethylamino)ethyl methacrylate (DMAEMA) on ODN complexation. Seeing that the work presented herein focuses on different aspects of PICM self-assembly, namely on the effects of PEG chain length, number of cationic repeat units and nature of these units on the interactions of the polymers with the ODN, both studies nicely complement one another. Furthermore, this study systematically investigates for the first time PICMs containing AEMA, a monomer bearing primary amino groups, which we hypothesize will allow us to adjust the buffering capacity of the polymers and be beneficial for complex stability.

MATERIALS AND METHODS

Materials

A 20-mer antisense phosphorothioate oligodeoxyribonucleotide (ODN; 5′-GTTCTCGCTGGTGAGTTTCA) and its 5′-fluorescein-labeled derivative were supplied by Medicorp Inc. (Montreal, QC, Canada). AEMA HCl was obtained from Polysciences Inc. (Warrington, PA) and protected with bis(*tert*-butyl)dicarbonate as described previously (28). The product (AEMABoc) was purified by silica gel chromatography (ethyl acetate/hexanes; 50/50 *v/v*) prior to use. Polyethylene glycol monomethyl ether (MeO-PEG-OH; M_n=3,000) was provided by Nektar (Huntsville, AL). All other chemicals were purchased from Sigma-Aldrich (Oakville, ON, Canada) and used as received, except for the following: tetrahydrofuran (THF) was passed through PureSolv™ drying columns (Innovative Technologies, Newburyport, MA), triethylamine was dried over calcium hydride and purified by distillation, and DMAEMA was vacuum-distilled prior to polymerization.

Techniques

^{1}H NMR spectra were recorded on a Bruker NMR spectrometer operating at 400 MHz (Milton, ON, Canada). Solutions were either prepared in deuterated chloroform or in deuterated water. Gel permeation chromatography (GPC) measurements were performed in THF using an Alliance GPCV 2000 system (Waters, Milford, MA) equipped with a differential refractive index detector. Adequate molecular weight separation was achieved using three Waters Styragel columns (HT2, HT3 and HT5) in series at a flow rate of 1.0 ml/min and a temperature of 40°C. A calibration curve was obtained with near-monodisperse PEG standards. Elemental analysis was used to determine the molar content of amino groups per gram of polymer. The measurements were conducted in an oxidative atmosphere at 1,021°C using a thermal conductivity probe (Fisons Instruments EA 1108 C, H, N, S Elemental Analyzer, Beverly, MA). The mean hydrodynamic diameter, size distribution, and scattering intensity of the micelles were determined using a Malvern Autosizer 4800 equipped with a 488-nm uniphase argon-ion laser (Malvern Instruments, Worcestershire, UK). Measurements were performed in triplicate at a scattering angle of 90° and a temperature of 25°C. The CONTIN program was used to extract size distributions from the auto-correlation functions. Size measurements falling out of the particle size range of the instrument (*i.e.* >5,000 nm) are shown as qualitative information only.

Synthesis of Atom Transfer Radical Polymerization (ATRP) Macroinitiators

MeO-PEG-OH (M_n=2,000, 3,000, and 5,000) were converted to ATRP macroinitiators by reaction with 2-bromoisobutyryl bromide as reported elsewhere (28,32). Briefly, PEG was dissolved in anhydrous THF to a final concentration of 100 g/l and stirred for 15 min in the presence of triethylamine (10 eq). 2-Bromoisobutyryl bromide (4 eq) was then added dropwise and the reaction was carried out for 48 h at room temperature. The crude product was solubilized in dichloromethane and purified by successive washings with 10% HCl, 1 N NaOH, and brine. The organic phase was dried over magnesium sulfate and the ATRP macroinitiator precipitated in diethyl ether.

Synthesis of Cationic Block Copolymers

The polymerization reactions were carried out as follows: the PEG macroinitiator (1 eq) was solubilized in THF in one

flask while the monomers (DMAEMA and/or AEMABoc—10 to 40 eq), 1,4,7,10,10-hexamethyltriethylenetetramine (1.4 eq), Cu(I)Br (1 eq), and $Cu(II)Br_2$ (0.25 eq) were solubilized in THF in a second reactor. Both solutions were degassed for 20 min with argon. The polymerization was initiated by transferring the macroinitiator to the monomer mixture using a two-head syringe. In all cases, the final monomer concentration was set to 0.8 M. The reactions were typically conducted for 16 h at 65°C, after which the copper complexes were removed by filtration through a silica gel column. All polymer extracts containing AEMABoc were dissolved in 3 M HCl/EtOAc (50 mg/ml) and reacted for 1 h in order to cleave the Boc protecting groups. The reaction was stopped by diluting with water and washing twice with EtOAc. The aqueous phase (containing the protonated polymer) was collected, dialyzed for 48 h against water (molecular weight cut-off 6,000–8,000) and freeze-dried to afford purified polymer. Copolymers of DMAEMA were treated in an equivalent fashion whereby they were dissolved in 1.5 N HCl, washed twice with EtOAc and dialyzed against water.

Potentiometric Titrations

Apparent pK_a values were calculated from the titration curves of the copolymers as described previously (28). pK_as were then used to determine the buffering capacity (β) of the copolymers at pH 5.5 according to Eq. 1.

$$\beta = 2.3 C_m \frac{K_a[H_3O^+]}{\left(K_a + [H_3O^+]^2\right)} \quad (1)$$

The pH value of 5.5 was selected to mimic a transfection experiment wherein the complexes would have been internalized *via* endocytosis. The concentration C_m then refers to the methacrylate monomer concentration (*i.e.* AEMA + DMAEMA) that would be found in the endosome. Assuming that typical transfection experiments are efficiently performed at 200 nM ODN (*i.e.* 2.75 μg/ml) (33) and that ideal PICMs are obtained at a nitrogen-to-phosphate (N/P) ratio of 1.5, C_m becomes 1.14×10^{-5} M.

Incorporation of ODN (Gel Electrophoresis)

PICMs were prepared in 10 mM Tris, pH 7.4 at N/P ratios varying from 0.5 to 3 using an ODN solution spiked with fluorescein-labeled ODN (25 mol%). Samples were mixed with glycerol and loaded onto a 20% (*w/v*) acrylamide gel prepared with a tris-borate-ethylenediaminetetraacetic acid (EDTA) buffer adjusted to pH 7.4. Following migration, the ODN was visualized by UV irradiation using a Chem-iImager 5500 imaging system (Alpha Innotech Corp., San Leandro, CA).

Micelle Formation as Ascertained by Dynamic Light Scattering (DLS)

Effect of N/P Ratio

Specific amounts of a copolymer solution (2–3 mg/ml) were added to a solution of ODN (0.1 mg/ml) in 10 mM Tris, pH 7.4 to yield complexes with N/P ratios varying from 0 to 3. DLS analyses were performed 45 min after each incremental addition of polymer. Both the stock polymer and ODN solutions were passed through 0.22-μm nylon filters prior to experimentation.

Effect of Ionization Degree

PICMs of PEG_{68}-*b*-$PDMAEMA_{25}$ were prepared in 10 mM Tris, pH 6.9 at an N/P ratio of 1.5 (final ODN concentration of 0.1 mg/ml). Both the stock polymer and ODN solutions were passed through 0.22-μm nylon filters prior to experimentation. Size measurements were compared to those obtained above for PEG_{68}-*b*-$PDMAEMA_{25}$ and PEG_{68}-*b*-$PAEMA_{26}$ at pH 7.4 and N/P ratio of 1.5.

Stability of Micelles by a Displacement Assay

PICMs were prepared in 10 mM Tris, pH 7.4 at an N/P ratio of 1.5 (final ODN concentration of 2.75 μg/ml) and incubated at room temperature for 30 min in presence of ethidium bromide (EtBr) (1 eq per base pair). Increasing amounts of low molecular weight heparin (sodium salt from porcine intestinal mucosa, MW of ~3,000 g/mol) were then added and the complexes incubated for an additional 75 min. The fluorescence of free EtBr (F_i), ODN/EtBr (F_o), and EtBr/PICM after addition of heparin (F_h) was recorded on a Safire plate reader (Tecan, Medford, MA; λ_{ex}=523 nm, λ_{em}=587 nm). Relative fluorescence values were calculated from Eq. 2:

$$\text{Relative fluorescence} = \frac{(F_h - F_i)}{(F_o - F_i)} \times 100 \quad (2)$$

An increase in relative fluorescence is indicative of the destabilization of the micelles.

Protection Against DNAse I Degradation

The ability of the PICMs to protect the ODN against enzymatic degradation was evaluated as described previously (34). PICMs were prepared at an N/P ratio of 1.5 using an ODN solution spiked with 50 mol% fluorescein-labeled ODN (final ODN concentration of 44 μg/ml). The complexes (as

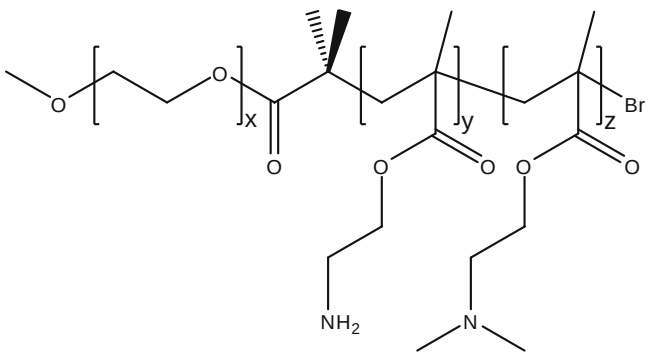

Fig. 1. Structure of the copolymers studied where *x* corresponds to the number of ethylene oxide (EO) repeat units while *y* and *z* correspond to the number of AEMA and DMAEMA methacrylate units, respectively. The value *x* is equal to 45, 68 or 113 for PEG 2,000, 3,000 or 5,000, respectively, while *y* and *z* vary between 0 and 40.

Table I. Characteristics of the Copolymers of the AEMA Series

	GPC[b]			^{1}H NMR		Elemental analysis	
Copolymer[a]	M_n	M_w	PI	M_n[c]	Nitrogen content[c] (mol/g polymer) $\times 10^3$	Nitrogen weight %	Nitrogen content[c] (mol/g polymer) $\times 10^3$
PEG_{45}-*b*-$PAEMA_{12}$	3,100	3,800	1.23	4,200	2.93	4.01	2.86
PEG_{45}-*b*-$PAEMA_{23}$	4,500	5,900	1.31	5,900	3.83	5.23	3.73
PEG_{45}-*b*-$PAEMA_{28}$	5,300	7,000	1.33	6,800	4.12	5.73	4.09
PEG_{45}-*b*-$PAEMA_{35}$	6,000	8,100	1.35	7,900	4.39	6.07	4.33
PEG_{45}-*b*-$PAEMA_{41}$	6,600	8,800	1.33	8,900	4.57	6.29	4.49
PEG_{68}-*b*-$PAEMA_{13}$	4,400	5,200	1.18	5,200	2.39	3.35	2.39
PEG_{68}-*b*-$PAEMA_{20}$	5,200	6,100	1.18	6,500	3.09	4.24	3.03
PEG_{68}-*b*-$PAEMA_{26}$	6,200	7,000	1.14	7,500	3.48	4.62	3.30
PEG_{68}-*b*-$PAEMA_{30}$	6,400	7,400	1.17	8,200	3.70	5.01	3.58
PEG_{68}-*b*-$PAEMA_{38}$	7,100	8,500	1.20	9,500	4.02	5.44	3.88
PEG_{113}-*b*-$PAEMA_{11}$	6,200	7,300	1.17	7,000	1.59	2.21	1.58
PEG_{113}-*b*-$PAEMA_{17}$	6,900	8,100	1.17	8,000	2.17	2.92	2.09
PEG_{113}-*b*-$PAEMA_{21}$	7,500	9,000	1.20	8,700	2.45	3.44	2.46
PEG_{113}-*b*-$PAEMA_{31}$	8,000	9,700	1.21	10,300	3.03	4.10	2.93
PEG_{113}-*b*-$PAEMA_{36}$	8,800	10,500	1.19	11,200	3.25	4.36	3.11

[a] Copolymers are labeled as PEG_x-*b*-$PAEMA_y$ where *x* is the number of EO repeat units based on PEG MW and *y* is the number of methacrylate repeat units determined by ^{1}H NMR.
[b] GPC data is for the protected (Boc) crude copolymers prior to purification.
[c] M_n by ^{1}H NMR and nitrogen content (both by ^{1}H NMR and elemental analysis) were calculated assuming full ionization of the monomer (*i.e.* MW=166.6 g/mol for the hydrochloride salt of AEMA).

well as a control solution of ODN) were incubated with DNAse I (≥2,000 kU/mg protein activity, used at a 50 U/μg ODN concentration) in presence of 5 mM $MgCl_2$ at 37°C for pre-determined periods of time. Degradation was stopped by addition of EDTA (final concentration of 8.3 mM) and the ODN freed in presence of an excess heparin. Samples were then treated with formamide and loaded onto a 20% (*w/v*) acrylamide gel. The ODN was visualized by UV irradiation and the amount of intact ODN quantified relative to the signal of an intact ODN sample.

RESULTS AND DISCUSSION

Polymer Synthesis

A library of polymers with varying hydrophilic (PEG MW of 2,000, 3,000 and 5,000) and cationic (10–40 monomeric units) block lengths was prepared in order to shed light on the effects of polymer composition on PICM self-assembly. The nature of the amino group was also varied using AEMA—a primary amine, DMAEMA—a tertiary amine, and their

Table II. Characteristics of the Copolymers of the DMAEMA Series

	GPC[b]			^{1}H NMR		Elemental analysis	
Copolymer[a]	M_n	M_w	PI	M_n[c]	Nitrogen content[c] (mol/g polymer) $\times 10^3$	Nitrogen weight %	Nitrogen content[c] (mol/g polymer) $\times 103$
PEG_{45}-*b*-$PDMAEMA_{13}$	2,800	3,400	1.2	4,600	2.76	3.76	2.69
PEG_{45}-*b*-$PDMAEMA_{23}$	3,600	4,300	1.18	6,500	3.47	4.48	3.20
PEG_{45}-*b*-$PDMAEMA_{28}$	4,000	4,700	1.18	7,500	3.69	4.69	3.35
PEG_{45}-*b*-$PDMAEMA_{34}$	4,400	5,200	1.17	8,700	3.90	5.04	3.59
PEG_{45}-*b*-$PDMAEMA_{40}$	4,900	5,900	1.18	9,800	4.04	5.20	3.71
PEG_{68}-*b*-$PDMAEMA_{13}$	4,000	4,700	1.18	5,600	2.25	3.05	2.18
PEG_{68}-*b*-$PDMAEMA_{20}$	4,500	5,200	1.15	6,900	2.82	3.86	2.76
PEG_{68}-*b*-$PDMAEMA_{25}$	4,800	5,600	1.16	8,000	3.12	4.13	2.95
PEG_{68}-*b*-$PDMAEMA_{31}$	5,400	6,300	1.17	9,100	3.37	4.48	3.20
PEG_{68}-*b*-$PDMAEMA_{35}$	5,600	6,700	1.19	9,800	3.51	4.54	3.24
PEG_{113}-*b*-$PDMAEMA_{10}$	5,200	5,800	1.12	7,000	1.40	2.06	1.50
PEG_{113}-*b*-$PDMAEMA_{17}$	5,800	6,700	1.15	8,400	2.01	2.74	1.96
PEG_{113}-*b*-$PDMAEMA_{23}$	6,500	7,700	1.17	9,600	2.41	3.26	2.33
PEG_{113}-*b*-$PDMAEMA_{27}$	6,900	8,500	1.22	10,400	2.62	3.48	2.48
PEG_{113}-*b*-$PDMAEMA_{33}$	7,300	8,700	1.19	11,500	2.85	3.83	2.74

[a] Copolymers are labeled as PEG_x-*b*-$PDMAEMA_z$ where *x* is the number of EO repeat units based on PEG MW and *z* is the number of methacrylate repeat units determined by ^{1}H NMR.
[b] GPC data is for the crude copolymers prior to purification.
[c] M_n by ^{1}H NMR and nitrogen content (both by ^{1}H NMR and elemental analysis) were calculated assuming full ionization of the monomer (*i.e.* MW=193.7 g/mol for the hydrochloride salt of DMAEMA).

Table III. Characteristics of the AEMA/DMAEMA Copolymers

Copolymer[a]	GPC[b]			^{1}H NMR		Elemental analysis		Titration	
	M_n	M_w	PI	M_n[c]	Nitrogen content[c] (mol/g polymer) $\times 10_3$	Nitrogen weight %	Nitrogen contents[c] (mol/g polymer) $\times 10_3$	pK_a	Buffering capacity (mol/L) $\times 10^6$
PEG_{68}-*b*-$PAEMA_{26}$	6,200	7,000	1.14	7,500	3.48	4.62	3.30	6.95	0.43
PEG_{68}-*b*-P($AEMA_{19}$-*co*-$DMAEMA_5$)	5,500	6,700	1.20	7,300	3.29	4.44	3.17	6.78	0.62
PEG_{68}-*b*-P($AEMA_{13}$-*co*-$DMAEMA_{12}$)	5,700	6,700	1.17	7,600	3.26	4.25	3.03	6.64	0.82
PEG_{68}-*b*-P($AEMA_6$-*co*-$DMAEMA_{19}$)	5,100	5,800	1.13	7,800	3.19	4.16	2.97	6.54	1.00
PEG_{68}-*b*-$PDMAEMA_{25}$	4,800	5,600	1.16	8,000	3.12	4.13	2.95	6.51	1.06

[a] Copolymers are labeled as PEG_x-*b*-P($AEMAy$-*co*-$DMAEMA_z$) where *x* is the number of EO repeat units based on PEG MW and y and *z* are the numbers of methacrylate repeat units determined by ^{1}H NMR.
[b] GPC data is for the protected (Boc) crude copolymers prior to purification.
[c] M_n by ^{1}H NMR and nitrogen content (both by ^{1}H NMR and elemental analysis) were calculated assuming full ionization of the monomer (*i.e.* MW=166.6 g/mol and MW=193.7 g/mol for the hydrochloride salts of AEMA and DMAEMA, respectively).

mixtures to adjust the buffering capacity of the cationic segment. The structures of the various copolymers are depicted in Fig. 1 while the details of their compositions are presented in Tables I, II and III.

The block copolymers were prepared by ATRP from a PEG macroinitiator, as described previously (28). In this case, however, $CuBr_2$ was used to favor the formation of diblock copolymers. Indeed, as suggested by Lenoir *et al.*, the presence of Cu(II) salts slows down the propagation rate in comparison to the initiation rate, thereby increasing the initiation efficiency (35). Addition of $CuBr_2$ turned out to be particularly crucial for the synthesis of the copolymers with the shortest cationic chains. The shift of the GPC polymer peak to higher MW and the presence of a unimodal MW distribution both suggest that diblock copolymers were indeed obtained (data not shown). Polymers with polydispersity indices (PI) within the 1.15–1.3 range were typically found.

The cationic block length was controlled by increasing the monomer/macroinitiator ratio. The polymer composition was determined by ^{1}H NMR by comparing the intensity of the peaks of the cationic segment (peaks at ~4.0 ppm (2H) or ~2.6 ppm (2H) corresponding to the methylene groups of the pendant chain of the methacrylate monomers) to that of the PEG block (3.64 ppm; peak of known intensity based on MW). The polymer composition was confirmed by elemental analysis based on the nitrogen weight content of the copolymers. Results by ^{1}H NMR and elemental analysis correlated well yet a small discrepancy was obtained; the nitrogen contents obtained by elemental analysis were systematically lower than those calculated by ^{1}H NMR. The greatest difference observed was for the copolymers of the DMAEMA series and never exceeded 9%. This can be explained by the combined effects of the presence of trace water (affecting elemental analysis data) and uncertainties on both the intensity of the PEG ^{1}H NMR peak and on the real ionization degree of the amine-containing units.

Polymers with mixtures of AEMA and DMAEMA were further characterized by titration to determine their pK_a and to establish potential correlations between ionization degree and interaction with ODN. It is shown that the pK_a decreases from 6.95 to 6.51 as the fraction of DMAEMA increases over that of AEMA (Table III). In parallel, copolymers with the tertiary amine (DMAEMA) present a 2.4-fold increase in buffering capacity compared to those with the primary amine (AEMA). A closer look at the data reveals that the buffering capacity can be fine tuned by varying the relative amount of the two cationic monomers.

Effect of N/P Ratio on Micelle Formation

Incorporation of ODN

Complete incorporation of the ODN in the complexes can be evidenced by gel electrophoresis through both the disappearance of the migration band corresponding to the free ODN and a decrease in the fluorescence signal of the ODN (due to self-quenching following incorporation of the fluorophore in the core of the micelles). As can be seen in Fig. 2A–C for the copolymers of the AEMA series, complete

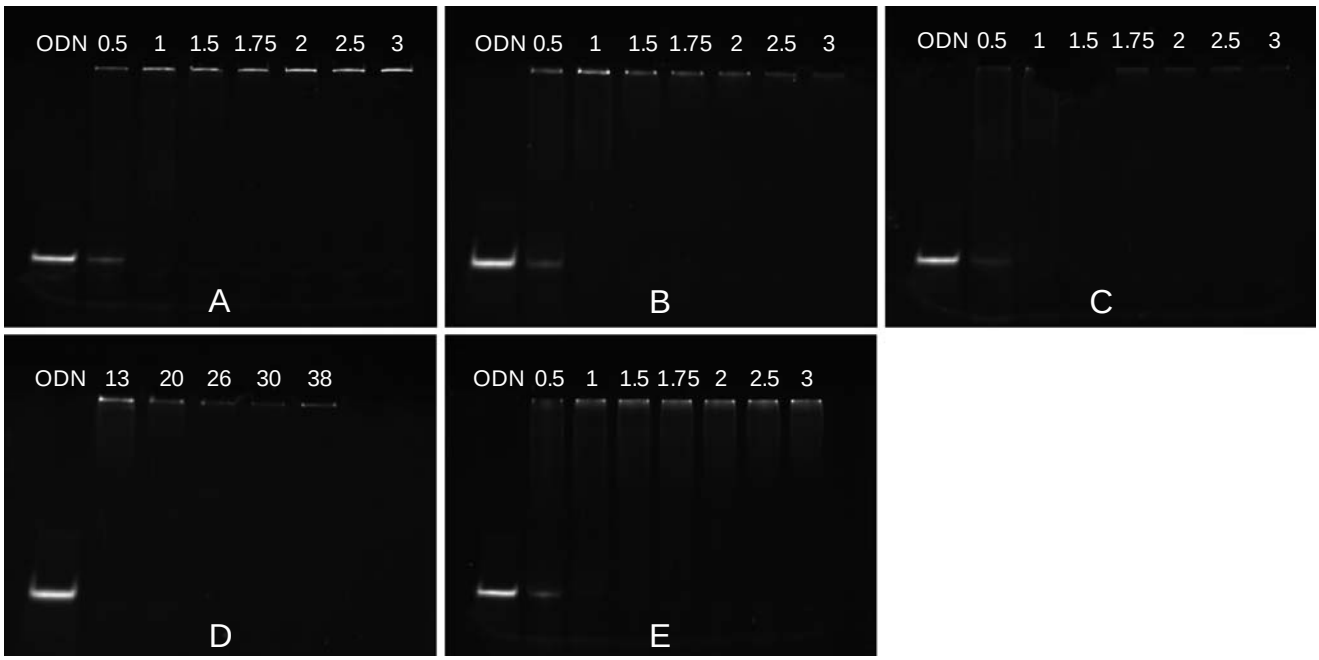

Fig. 2. Gel electrophoresis of PICMs prepared at N/P ratios varying from 0.5 to 3 using PEG_{45}-*b*-$PAEMA_{23}$ (**A**), PEG_{68}-*b*-$PAEMA_{20}$ (**B**), PEG_{113}-*b*-$PAEMA_{21}$ (**C**) and PEG_{68}-*b*-$PDMAEMA_{20}$ (**E**). PICMs prepared at the fixed N/P ratio of 1.75 using polymers of the PEG_{68}-*b*-AEMA series with increasing cationic block lengths are also shown (**D**).

incorporation of the ODN occurs at an N/P ratio of 1. At this ratio, however, a smeared band is still observed at high MW, corresponding to partially neutralized complexes. As the N/P ratio increases, this band progressively disappears, suggesting that all negative charges are effectively complexed. Comparison of Fig. 2A–C further indicates that the presence of increasingly long PEG segments does not hamper ODN complexation. This is in line with the results of Deshpande *et al.* who have shown good ODN binding of all their PEG/DMAEMA polymers, irrespective of architecture (31).

The effect of the cationic block length on ODN incorporation was also studied by preparing micelles at the N/P ratio of 1.75 with polymers of the PEG_{68}-*b*-PAEMA series (Fig. 2D). As can be seen, all polymers were able to efficiently complex the ODN. However, a smeared band at high MW was observed for the copolymers with the lowest number of cationic repeat units. This band eventually disappeared as the number of cationic units reached 26, suggesting that increased cooperativity leads to more efficient interaction with the ODN.

A similar general behavior was observed for the copolymers of the DMAEMA series (results for PEG_{68}-*b*-$PDMAEMA_{20}$ are presented in Fig. 2E). For those polymers, complete ODN incorporation also occurred at the N/P ratio of 1 despite the differences in pK_a and ionization degree between DMAEMA and AEMA. Rungsardthong *et al.* have reported an analogous behavior for calf thymus DNA/DMAEMA complexes prepared from PDMAEMA of decreasing ionization degree (*i.e.* prepared at pHs 4.0, 6.0, 7.4 and 8.0) (36). It was shown that even at high pH the complexes interacted stoichiometrically with the DNA. This was attributed to the fact that the presence of a strong acid like DNA could induce the protonation of the weak cationic DMAEMA units. Our results further evidence differences between the complexes of AEMA and DMAEMA, with smearing still observed at the high N/P ratio of 3 for DMAEMA (Fig. 2E). The presence of smeared bands at high N/P ratios suggests that complexes based on DMAEMA are less stable than those based on AEMA; the stability of the complexes will be studied in more details later in the manuscript.

Colloidal Properties

The effect of the N/P ratio on the colloidal properties of the micelles was also studied and is presented in Fig. 3 for the copolymer PEG_{68}-*b*-$PAEMA_{26}$. A first observation (valid for all polymers) is that the scattering intensity increases as the N/P ratio reaches 1.5 and then slowly decreases at higher N/P ratios. For PEG_{68}-*b*-$PAEMA_{26}$, the increase in scattering intensity correlates with larger sizes (compare sizes close to 1.5 *vs.* at low N/P ratios) and probably follows from an increase in the hydrophobicity of the AEMA segment due to complete charge compensation. However, for polymers having high ethylene oxide (EO)/cationic balances, and therefore greater levels of steric stabilization, this increase in size is not significant and cannot justify the observed increase in scattering intensity (data not shown). Another reasonable explanation is that as more polymer is added to go from low N/P ratios to ratios closer to neutrality, the number of micelles increases, leading to higher scattering intensity. Alternatively, Dautzenberg *et al.* have shown that the maximum in scattering intensity was associated with an increase in the mean polymer weight fraction of individual PICMs, reflecting an increase in the density or compactness of the micelles (37). It is therefore suggested that the increase in scattering intensity observed here at the N/P ratio of 1.5 is

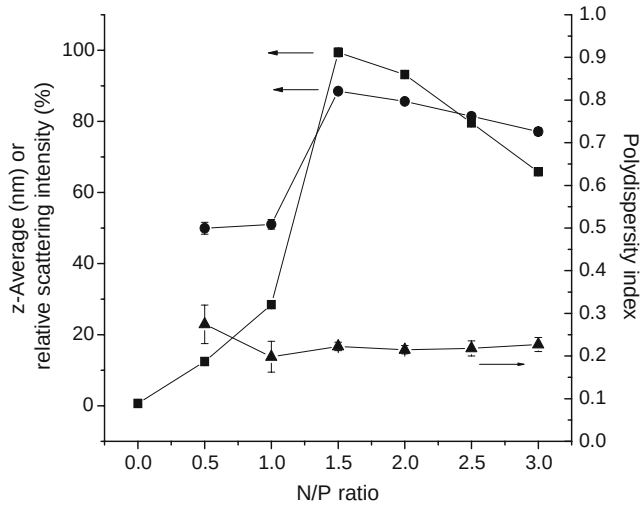

Fig. 3. Colloidal properties of PEG_{68}-*b*-$PAEMA_{26}$ micelles prepared at N/P ratios varying from 0.5 to 3. Effects of N/P ratio on average diameter (*z*-Average; *filled circle*), scattering intensity (*filled square*) and PI (*filled triangle*) are shown. Mean ± standard deviation (SD) (n=3).

due to the combined effects of the number of micellar assemblies and of hydrophobicity on size and density of the micelles.

Although admittedly not striking in Fig. 3, another important finding of these experiments is that the evolution of the PI with N/P ratio follows an opposite trend to that of scattering intensity, *i.e.* PI is minimal at N/P ratios of 1–1.5 and slowly increases when departing from that range. This trend was paralleled with the tendency of micelles prepared at N/P ratios below and above 1.5 to present multi-modal size distributions (data not shown). This phenomenon was particularly significant for polymers having low EO/cationic unit balances (sterically less stable).

Effect of Polymer Composition and Length on Micelle Formation

The effects of the PEG chain length, number of cationic monomeric units and nature of the amino group on micelle properties were further studied at the N/P ratio of 1.5 and are summarized in Fig. 4A. By comparing the traces for the polymers of the PEG_{45}-*b*-PAEMA, PEG_{68}-*b*-PAEMA and PEG_{113}-*b*-PAEMA series (filled symbols), it is clearly seen that the size of the complexes decreases as the PEG chain length increases. This trend falls in line with what was observed for other polyelectrolyte complexes (27,38) and can be attributed to the increased steric hindrance associated with the longer PEG blocks. The hydrophilic chains indeed become bulkier as their length increases so that the micelles are constrained to adopt a conformation that maximizes the space between the hydrophilic segments. This occurs when the micelles present a higher radius of curvature, *i.e.* when the core of the micelles is smaller. Although not shown here, a comparable behavior was observed when comparing polymers of the PEG_{45}-*b*-PDMAEMA, PEG_{68}-*b*-PDMAEMA and PEG_{113}-*b*-PDMAEMA series.

A closer look at the data within each polymer series reveals that the size of the PICMs increases as the number of core-forming monomeric units increases (*e.g.* from 22 to 43 nm for polymers of the PEG_{113}-*b*-PAEMA series). This trend comes as no surprise and was reported previously for other polyelectrolyte complexes (38–40). Of interest is the fact that there seems to be a critical EO/cationic unit balance that needs to be reached in order to achieve colloidal stability. Indeed, multi-modal size distributions, and in some cases macroscopic aggregation, were observed for samples of the PEG_{45}-*b*-PAEMA series having 23 cationic units and more and for samples of the PEG_{68}-*b*-PAEMA series having 30 cationic units and more. This corresponds to EO/AEMA ratios of 2.0 and 2.3, respectively (or to nitrogen densities of 3.83×10^{-3} and 3.70×10^{-3} mol nitrogen/g of polymer, respectively). This critical ratio is never reached for polymers of the PEG_{113}-*b*-PAEMA series so that unimodal and relatively monodisperse (PI of ~0.14) micelles are obtained throughout. Aggregation of the PICMs as the cationic block length increases can be rationalized by an increase in the likelihood of interpolymer bridgings (chain entanglements) to take place between the micelles.

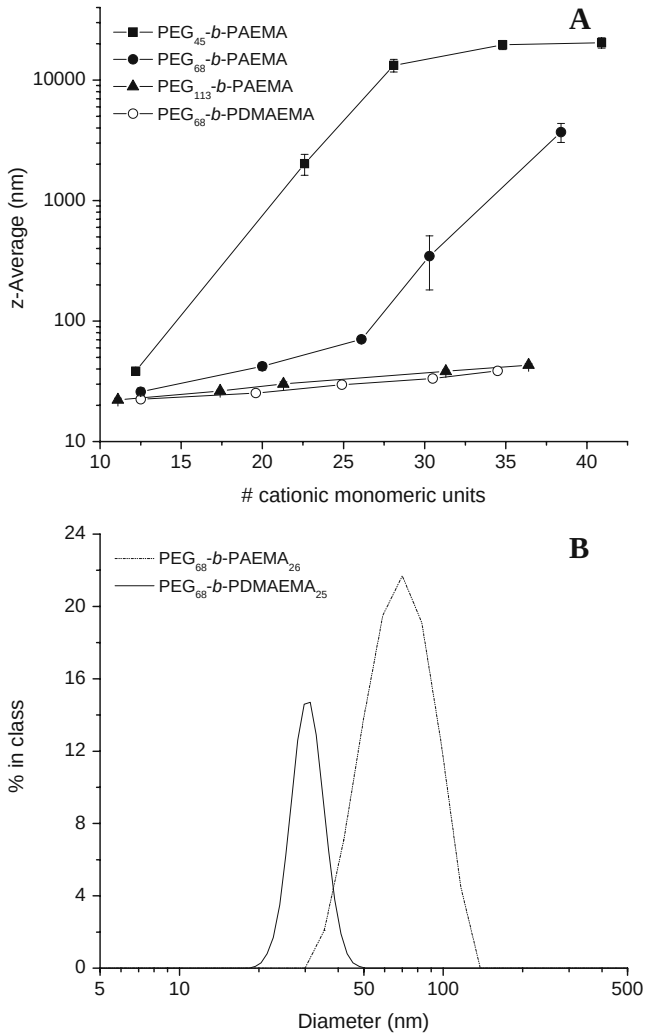

Fig. 4. Average diameter (*z*-average) of PICMs prepared at the N/P ratio of 1.5. Mean ± SD (n=3) is shown (**A**). Typical size distributions of micelles of PEG_{68}-*b*-$PDMAEMA_{25}$ and PEG_{68}-*b*-$PAEMA_{26}$ are also presented (**B**).

Alternatively, it can be argued that an increase in the number of cationic units will shift the EO/hydrophobic balance of the charged-compensated segments such that the PEG chains are no longer able to impart solubility to the micelles. Aggregated particles then result from hydrophobic–hydrophobic interactions between exposed neutral cores.

The effect of the nature of the amino group on the properties of the PICMs can finally be evidenced from Fig. 4 for PEG_{68} copolymers (compare traces with filled and empty circle symbols). It appears that going from the cationic unit AEMA to the DMAEMA unit leads to a decrease in size from ~70 to 30 nm and a decrease in PI from 0.20 to 0.10 (compare size distributions in Fig. 4B). This trend could follow from the different ionization degrees of the polymers (37% for AEMA *vs.* 24% for DMAEMA at pH 7.4). To evaluate the contribution of ionization degree on micelle size, PICMs of PEG_{68}-*b*-$PDMAEMA_{25}$ were prepared in 10 mM Tris pH 6.9 and compared to those of PEG_{68}-*b*-$PAEMA_{26}$ obtained at pH 7.4. At pH 6.9, the DMAEMA units are ionized to the same extent as the AEMA units at pH 7.4. The size of the DMAEMA micelles did not considerably change from pH 7.4 to pH 6.9 (data not shown), suggesting that such small variations in ionization degree do not contribute to the differences observed between AEMA and DMAEMA. Another explanation could be that the presence of two extra methyl groups on the amino group of DMAEMA hinders the fit and the interaction between the cation and the phosphate groups of the ODN (24). The interactions between the ODN and the AEMA units would be comparatively stronger, leading to seemingly more hydrophobic segments and possibly higher aggregation numbers (and micellar diameters).

Effect of Polymer Composition and Length on the Stability of Micelles Towards Dissociation

In those experiments, the micelles were incubated with an anionic macromolecule that can typically be found in the blood stream (heparin). Both the ODN and heparin can interact with the cationic polymer and a competition for the cationic sites is therefore set. At high enough concentrations, heparin will eventually occupy all cationic sites, thereby expelling the ODN out of the micellar system. If on the basis of colloidal properties alone it appeared that long PEG chains and short cationic blocks were advantageous, an opposite trend was found when studying the stability of the PICMs towards dissociation. Figure 5A shows that the longer the PEG chain is, the less stable the micelles. This can be understood considering that a longer PEG chain results in polymers with a higher hydrophilic/hydrophobic balance and expectedly higher critical aggregation concentrations. For those polymers, the concentration of unmicellized charge-compensated uni/oligomers, which are more accessible for displacement by heparin, is higher. Destabilization by another polyanion therefore becomes easier as the PEG length increases. This is evidenced with twice as much fluorescence recovered in the case of PEG 5000 compared to PEG 2000-based micelles (Fig. 5A). Alternatively, an increase in the cationic block length results in additional cooperative interactions and in stronger binding (41). The effect on PICM stability towards dissociation is that the micelles become more stable as the number of cationic repeat units increases

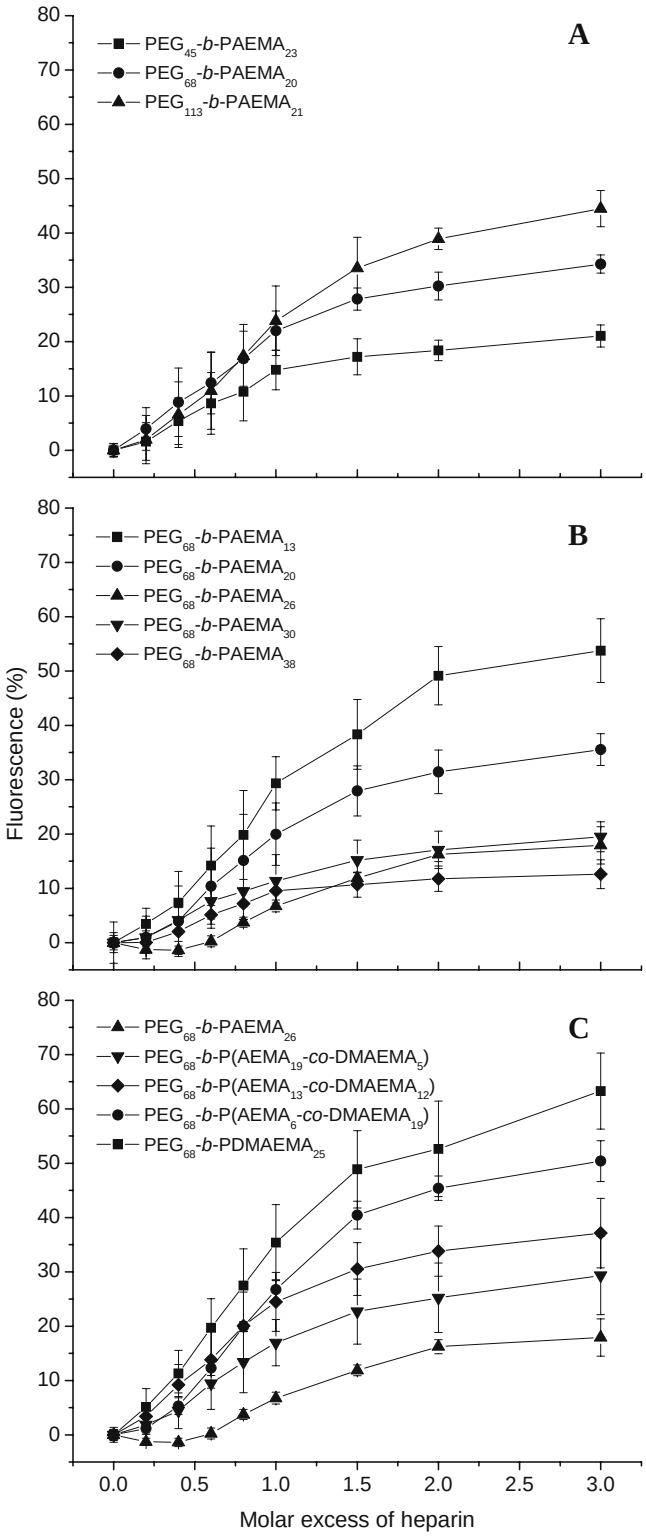

Fig. 5. Destabilization of micelles in presence of the competitive polyanion heparin. The effects of the PEG chain length (**A**), number of cationic monomeric units (**B**) and nature of the amino group (**C**) on PICM stability are shown. An increase in fluorescence is indicative of the release of entrapped ODN and of the destabilization of the micelles. Mean ± SD (n=3).

(Fig. 5B). Interestingly, a critical EO/cationic unit ratio for optimal stability is also observed, *i.e.* decreasing the EO/cationic unit ratio below 2.6 does not additionally contribute to the stability of the micelles. This correlates to the situation where micellar aggregation was observed (Fig. 4A). Finally, while copolymers of DMAEMA lead to nicely distributed micelles, they concomitantly produce assemblies vulnerable to competition and dissociation, with up to 63% fluorescence recovered compared to 17% for similar copolymers of AEMA (Fig. 5C). This suggests stronger interactions between the AEMA segments and the ODN. As postulated above, increased interactions could follow from a better fit between the cationic groups of AEMA and the phosphate groups of the ODN. The results of Fig. 5C further show that it is possible to adjust the stability of the micelles simply by varying the relative proportion of the primary *vs.* tertiary amines of the polymer. Indeed, intermediate properties are found for copolymers with both AEMA and DMAEMA.

Effect of Polymer Composition and Length on Protection of the ODN Against DNAse I Degradation

In the previous section, correlations between polymer composition, PICM stability and release of ODN from the assemblies were established. Similar trends were expected to follow regarding the ability of the micelles to protect the ODN against enzymatic degradation. Indeed, Elsabahy *et al.* have shown that PICMs composed of a PEG–ODN conjugate and higher generations of polyamidoamine dendrimers were not only increasingly stable against dissociation but could protect the ODN more efficiently against enzymatic degradation (42). Likewise, they showed that decreasing the PEG chain length from 20,000 to 10,000 helped protecting the ODN.

In the present manuscript, the DNAse I concentration was adjusted so that degradation of the naked ODN would occur in the span of a few hours. As can be seen in Fig. 6 (star symbols), 62% of the naked ODN was degraded within 6 h of incubation with DNAse I. As expected, incorporation of the ODN in the core of micelles prevented the action of the enzyme. Surprisingly, all micellar systems protected the ODN to the same extent, regardless of the PEG chain length (panel A), the number of cationic monomeric units (panel B) and nature of the amino group (panel C). This could be explained by the fact that, in all cases, the DNAse I was unable to access the entrapped ODN, be it through the steric hindrance provided by the PEG chains or the protection ensured by complexation with the cationic segment.

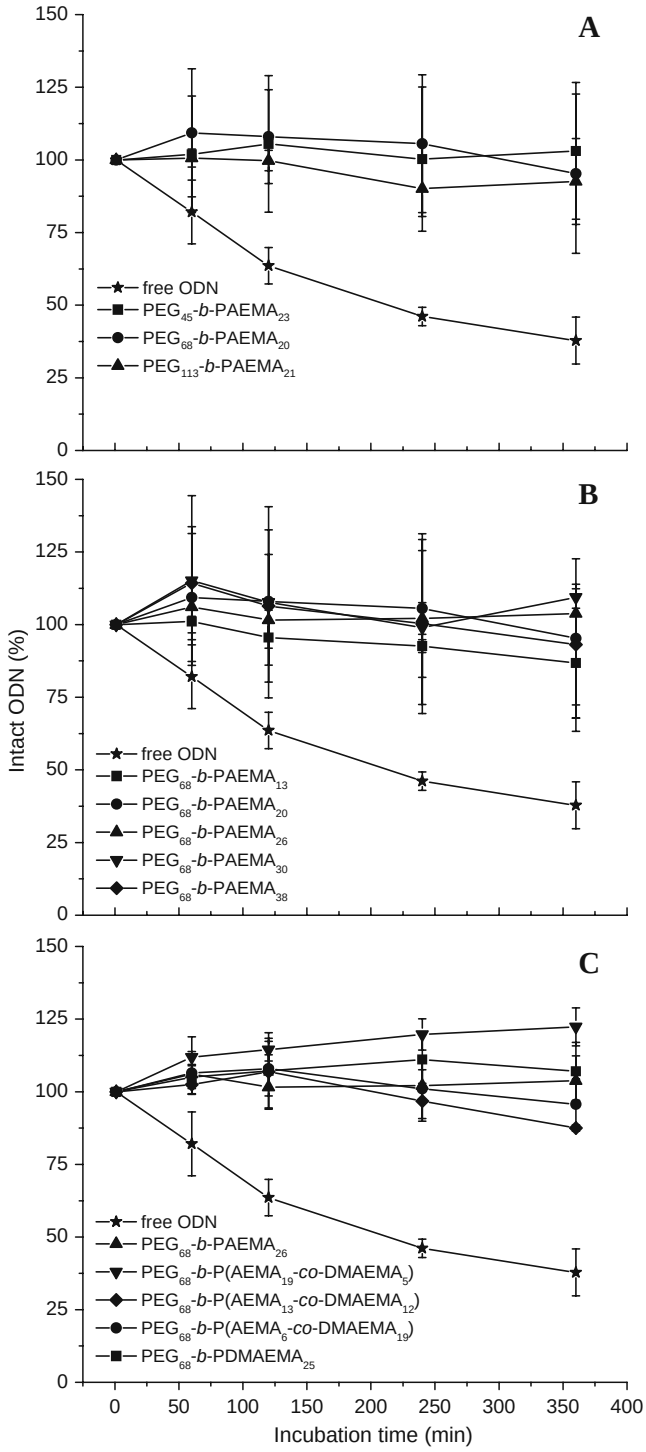

Fig. 6. The ability of the PICMs to protect the ODN against DNAse I degradation (50 U/μg ODN, 37°C, pH 7.4) is shown as a function of the PEG chain length (**A**), number of cationic monomeric units (**B**) and nature of the amino group (**C**) of the copolymers. Mean ± SD (n=3).

CONCLUSION

This work provides a systematic understanding of the effects of polymer composition on the properties of ODN-based micelles that should help rationally address the challenges of ODN delivery. For instance, the results show that if high stability is required, increased interactions between the polymer and ODN are desirable. This can be achieved either by augmenting the number of cationic units or by using AEMA as the cationic monomer. Alternatively, control over the size of the particles is possible by varying the EO/cationic unit ratio. In this case, an increase in the PEG chain length and the use of DMAEMA will both lead to smaller sizes and narrowly distributed micelles. Finally, if high buffering capacity is critical, the DMAEMA units should be favoured over the AEMA units.

With such information at hand, an evaluation of which copolymers should best address the challenges of ODN delivery can be attempted. The polymers of the PEG_{45}-*b*-PAEMA series show enhanced stability towards dissociation, which could prove advantageous considering the rapid dilution and exposure to blood components that will follow from intravenous injection. PICMs composed of PEG_{45}-*b*-PAEMA, however present sizes that may not be optimal for long circulating properties and passive targeting through the enhanced permeation and retention effect (43). Increasing the PEG chain length of the copolymers could solve this issue, but this will be at the cost of micelle stability. At the cellular level, the higher buffering capacity of the DMAEMA copolymers might be desirable to promote endosomal escape of the ODN *via* the so-called proton-sponge mechanism (44). Furthermore, assuming that their micelles can reach their target site intact, copolymers of the PEG_{113}-*b*-PDMAEMA series should be preferred since they present the lowest stability towards dissociation. In this case, low stability is desirable to increase the cytoplasmic/nuclear availability of the ODN (26).

Clearly, the physical requirements of a gene delivery system for overcoming both extracellular and intracellular barriers can be quite different so that the optimal polymer properties to fulfill one or another of the challenges of gene delivery can be opposing. Overall, copolymers of the type PEG_{68}-*b*-P(AEMA-*co*-DMAEMA) lead to micelles that present good colloidal properties, intermediate stability towards dissociation and adjustable buffering capacity, indicating that they are interesting polymers for future *in vitro* and *in vivo* studies.

ACKNOWLEDGMENTS

This work was financially supported by the Natural Sciences and Engineering Research Council of Canada (NSERC) and the Canada Research Chair Program. M.H. D. further acknowledges graduate research scholarships from NSERC and Fonds Québécois de la Recherche sur la Nature et les Technologies.

REFERENCES

1. B. A. Bunnell, and R. A. Morgan. Gene therapy for infectious diseases. *Clin. Microbiol. Rev* **11**:42–56 (1998).
2. I. A. McNeish, S. J. Bell, and N. R. Lemoine. Gene therapy progress and prospects: cancer gene therapy using tumour suppressor genes. *Gene Ther* **11**:497–503 (2004).
3. J. C. T. van Deutekom, and G. J. B. van Ommen. Advances in Duchenne muscular dystrophy gene therapy. *Nat. Rev. Genet* **4**:774–783 (2003).
4. S. Ferrari, D. M. Geddes, and E. W. F. W. Alton. Barriers to and new approaches for gene therapy and gene delivery in cystic fibrosis. *Adv. Drug Deliv. Rev* **54**:1373–1393 (2002).
5. S. Agrawal, J. Temsamani, and J.Y. Tang. Pharmacokinetics, biodistribution, and stability of oligodeoxynucleotide phosphorothioates in mice. *Proc. Natl. Acad. Sci. U. S. A* **88**:7595–7599 (1991).
6. E. Wickstrom. Oligodeoxynucleotide stability in subcellular extracts and culture media. *J. Biochem. Biophys. Methods* **13**:97–102 (1986).
7. A. Rifai, W. Brysch, K. Fadden, J. Clark, and K. H. Schlingensiepen. Clearance kinetics, biodistribution, and organ saturability of phosphorothioate oligodeoxynucleotides in mice. *Am. J. Pathol* **149**:717–725 (1996).
8. M. D. Hughes, M. Husssain, Q. Nawaz, P. Sayyed, and S. Akhtar. The cellular delivery of antisense oligonucleotides and ribozymes. *Drug Discov. Today* **6**:303–315 (2001).
9. J. Kurreck. Antisense tchnologies. Improvement through novel chemical modifications. *Eur. J. Biochem* **270**:1628–1644 (2003).
10. S. C. De Smedt, J. Demeester, and W. E. Hennink. Cationic polymer based gene delivery systems. *Pharm. Res* **17**:113–126 (2000).
11. E. Mastrobattista, M. A. E. M. van der Aa, W. E. Hennink, and D. J. A. Crommelin. Artificial viruses: a nanotechnological approach to gene delivery. *Nat. Rev. Drug Discov* **5**:115–121 (2006).
12. D. W. Pack, A. S. Hoffman, S. Pun, and P. S. Stayton. Design and development of polymers for gene delivery. *Nat. Rev. Drug Discov* **4**:581–593 (2005).
13. D. Putnam. Polymers for gene delivery across length scales. *Nat. Mater* **5**:439–451 (2006).
14. A. V. Kabanov, S. V. Vinogradov, Y. G. Suzdaltseva, and V. Y. Alakhov. Water-soluble block polycations as carriers for oligonucleotide delivery. *Bioconjugate Chem* **6**:639–643 (1995).
15. K. Kataoka, H. Togawa, A. Harada, K. Yasugi, T. Matsumoto, and S. Katayose. Spontaneous formation of polyion complex micelles with narrow distribution from antisense oligonucleotide and cationic block copolymer in physiological saline. *Macromolecules* **29**:8556–8557 (1996).
16. C. Plank, K. Mechtler, F. C. Szoka, and E. Wagner. Activation of the complement system by synthetic DNA complexes: a potential barrier for intravenous gene delivery. *Hum. Gene Ther* **7**:1437–1446 (1996).
17. M. Ogris, S. Brunner, S. Schuller, R. Kircheis, and E. Wagner. PEGylated DNA/transferrin–PEI complexes: reduced interaction with blood components, extended circulation in blood and potential for systemic gene delivery. *Gene Ther* **6**:595–605 (1999).
18. H. Petersen, P. M. Fechner, A. L. Martin, K. Kunath, S. Stolnik, C. J. Roberts, D. Fischer, M. C. Davies, and T. Kissel. Polyethylenimine-*graft*-poly(ethylene glycol) copolymers: influence of copolymer block structure on DNA complexation and biological activities as gene delivery system. *Bioconjugate Chem* **13**:845–854 (2002).
19. C. Brus, H. Petersen, A. Aigner, F. Czubayko, and T. Kissel. Physicochemical and biological characterization of polyethylenimine-graft-poly(ethylene glycol) block copolymers as a delivery system for oligonucleotides and ribozymes. *Bioconjugate Chem* **15**:677–684 (2004).
20. S. Mao, M. Neu, O. Germershaus, O. Merkel, J. Sitterberg, U. Bakowsky, and T. Kissel. Influence of polyethylene glycol chain length on the physicochemical and biological properties of poly (ethylene imine)-graft-poly(ethylene glycol) block copolymer/siRNA polyplexes. *Bioconjugate Chem* **17**:1209–1218 (2006).
21. S. Sundaram, L. K. Lee, and C. M. Roth. Interplay of polyethyleneimine molecular weight and oligonucleotide backbone chemistry in the dynamics of antisense activity. *Nucleic Acids Res* **35**:4396–4408 (2007).
22. S. Sundaram, S. Viriyayuthakorn, and C. M. Roth. Oligonucleotide structure influences the interactions between cationic polymers and oligonucleotides. *Biomacromolecules* **6**:2961–2968 (2005).
23. E. Ramsay, and M. Gumbleton. Polylysine and polyornithine gene transfer complexes: A study of complex stability and cellular uptake as a basis for their differential *in-vitro* transfection efficiency. *J. Drug Target* **10**:1–9 (2002).
24. P. van de Wetering, E. E. Moret, N. M. E. Schuurmans-Nieuwenbroek, M. J. van Steenbergen, and W.E. Hennink. Structure–activity relationships of water-soluble cationic methacrylate/methacrylamide polymers for nonviral gene delivery. *Bioconjugate Chem* **10**:589–597 (1999).
25. M. A. Wolfert, P. R. Dash, O. Nazarova, D. Oupicky, L. W. Seymour, S. Smart, J. Strohalm, and K. Ulbrich. Polyelectrolyte vectors for gene delivery: influence of cationic polymer on biophysical properties of complexes formed with DNA. *Bioconjugate Chem* **10**:993–1004 (1999).
26. C. Arigita, N. J. Zuidam, D. J. A. Crommelin, and W. E. Hennink. Association and dissociation characteristics of polymer/DNA complexes used for gene delivery. *Pharm Res* **16**:1534–1541 (1999).
27. J. K. W. Lam, Y. Ma, S. P. Armes, A. L. Lewis, T. Baldwin, and S. Stolnik. Phosphorylcholine-polycation diblock copolymers as

synthetic vectors for gene delivery. *J. Control. Release* **100**:293–312 (2004).
28. M. H. Dufresne, and J. C. Leroux. Study of the micellization behavior of different order amino block copolymers with heparin. *Pharm. Res* **21**:160–169 (2004).
29. M. H. Dufresne, M. A. Gauthier, and J. C. Leroux. Thiol-functionalized polymeric micelles: From molecular recognition to improved mucoadhesion. *Bioconjugate Chem* **16**:1027–1033 (2005).
30. W. H. Heath, A. F. Senyurt, J. Layman, and T. E. Long. Charged polymers *via* controlled radical polymerization and their implications for gene delivery. *Macromol. Chem. Phys* **208**:1243–1249 (2007).
31. M. C. Deshpande, M. C. Garnett, M. Vamvakaki, L. Bailey, S. P. Armes, and S. Stolnik. Influence of polymer architecture on the structure of complexes formed by PEG-tertiary amine methacrylate copolymers and phosphorothioate oligonucleotide. *J. Control. Release* **81**:185–199 (2002).
32. M. Ranger, M. C. Jones, M. A. Yessine, and J. C. Leroux. From well-defined diblock copolymers prepared by a versatile atom transfer radical polymerization method to supramolecular assemblies. *J. Polym. Sci., A, Polym. Chem* **39**:3861–3874 (2001).
33. M. A. Yessine, C. Meier, H. U. Petereit, and J. C. Leroux. On the role of methacrylic acid copolymers in the intracellular delivery of antisense oligonucleotides. *Eur. J. Pharm. Biopharm* **63**:1–10 (2006).
34. M. A. Yessine, M. H. Dufresne, C. Meier, H. U. Petereit, and J. C. Leroux. Proton-actuated membrane-destabilizing polyion complex micelles. *Bioconjugate Chem* **18**:1010–1014 (2007).
35. S. Lenoir, C. Pagnoulle, C. Detrembleur, M. Galleni, and R. Jerome. New antibacterial cationic surfactants prepared by atom transfer radical polymerization. *J. Polym. Sci., A, Polym. Chem* **44**:1214–1224 (2006).
36. U. Rungsardthong, T. Ehtezazi, L. Bailey, S. P. Armes, M. C. Garnett, and S. Stolnik. Effect of polymer ionization on the interaction with DNA in nonviral gene delivery systems. *Biomacromolecules* **4**:683–690 (2003).
37. H. Dautzenberg, C. Konak, T. Reschel, A. Zintchenko, and K. Ulbrich. Cationic graft copolymers as carriers for delivery of antisense-oligonucleotides. *Macromol. Biosci* **3**:425–435 (2003).
38. M. Glodde, S. R. Sirsi, and G. J. Lutz. Physiochemical properties of low and high molecular weight poly(ethylene glycol)-grafted poly(ethylene imine) copolymers and their complexes with oligonucleotides. *Biomacromolecules* **7**:347–356 (2006).
39. A. Harada, H. Togawa, and K. Kataoka. Physicochemical properties and nuclease resistance of antisense-oligonucleotides entrapped in the core of polyion complex micelles composed of poly(ethylene glycol)–poly(L-lysine) block copolymers. *Eur. J. Pharm. Sci* **13**:35–42 (2001).
40. C. W. Scales, F. Q. Huang, N. Li, Y. A. Vasilieva, J. Ray, A. J. Convertine, and C. L. McCormick. Corona-stabilized interpolyelectrolyte complexes of siRNA with nonimmunogenic, hydrophilic/cationic block copolymers prepared by aqueous RAFT polymerization. *Macromolecules* **39**:6871–6881 (2006).
41. J. Jin, J. C. Achenbach, S. P. Zhu, and Y. F. Li. Complexation of well-controlled low-molecular weight polyelectrolytes with antisense oligonucleotides. *Colloid Polym. Sci* **283**:1197–1205 (2005).
42. M. Elsabahy, M. Zhang, S. M. Gan, K. C. Waldron, and J. C. Leroux. Synthesis and enzymatic stability of PEGylated oligonucleotide duplexes and their self-assemblies with polyamidoamine dendrimers. *Soft Matter* **4**:294–302 (2008).
43. G. Gaucher, M. H. Dufresne, V. P. Sant, N. Kang, D. Maysinger, and J. C. Leroux. Block copolymer micelles: preparation, characterization and application in drug delivery. *J. Control. Release* **109**:169–188 (2005).
44. O. Boussif, F. Lezoualc'h, M. A. Zanta, M. D. Mergny, D. Scherman, B. Demeneix, and J. P. Behr. A versatile vector for gene and oligonucleotide transfer into cells in culture and *in vivo*: polyethylenimine. *Proc. Natl. Acad. Sci. U. S. A* **92**:7297–7301 (1995).